

Surfactant-Modified Wheat Straw: Preparation, Characterization and its Application for Methylene Blue Adsorption from Aqueous Solution

Ebrahimian Pirbazari A^{1,2*}, Hashemian SF² and Yousefi A²

¹Faculty of Fouman, College of Engineering, University of Tehran, Fouman 43516-66456, Iran

²Faculty of Caspian, College of Engineering, University of Tehran, Rezvanshahr 43861-56387, Iran

Abstract

This work reports on the development of organo-modified wheat straw (WS) adsorbent prepared by using sodium dodecyl sulfate (SDS) for removing methylene blue (MB), a model cationic dye, from aqueous solution. The samples were characterized by scanning electron microscope (SEM), nitrogen physisorption and Fourier transforms infrared spectroscopy (FT-IR). Batch adsorption experiments were carried out to remove MB from its aqueous solutions using SDS modified WS (SMWS). Analysis of adsorption results showed that the adsorption pattern on the SMWS can be described perfectly with Langmuir isotherm model compared with Freundlich isotherm model, and the Langmuir adsorption capacity, Q_{max} was found to be 126.60 mg g⁻¹ for SMWS and 55 mg g⁻¹ for WS at 303K respectively. The adsorption kinetic followed the pseudo-second order kinetic model. Desorption studies suggest that MB adsorption onto the SMWS should be mainly controlled by the hydrophobic interaction mechanism, along with a considerable contribution of the cationic exchange mechanism.

Keywords: Wheat straw; Sodium dodecyl sulfate; Methylene blue; Adsorption; Isotherm; Kinetic; Mechanism

Introduction

Nowadays, with the rapid development of modern industries, the problem of water pollution has become increasingly serious [1]. Among all contaminants contained in industrial sewage, dyes are the most undesired ones for both toxicological and esthetical reasons [2,3]. Methylene blue (MB) is the most commonly used substance for dyeing cotton, wood and silk. However, MB can cause eye burns which may be responsible for permanent injury to eyes of human and animals [4]. Furthermore, MB can also increase heart rate, vomiting, shock, Heinz body formation, cyanosis, jaundice, and tissue necrosis in humans [5]. Some biological and physical/chemical methods have been employed for dye wastewater treatment. These methods include anaerobic/aerobic treatment [6], coagulation/flocculation [7], oxidation [8], ozonation [9], photocatalytic oxidation [10,11], membrane separation [12] and adsorption [13]. In all these methods, the adsorption has been found to be economical and effective dye wastewater treatment technique as it can remove various dyes with lower treatment cost. At present, there is a growing interest in using low cost adsorbents for dye adsorption. If an adsorbent is inexpensive and ready for use, the adsorption process will be a promising technique. Recently, some crude lignocellulosic materials had been used as low cost adsorbents.

Wheat straw, as a type of abundant agriculture waste in Iran, is rich in various natural polymers, such as cellulose and lignin, providing the chance of becoming a sort of adsorbents through chemical modification. However, the general treatment to the excess straws in Iran is still incineration until now, which is not only destruction of the atmospheric environment, but waste of resources. In recent years, straw based adsorbents have been already paid more attention in water purification, as they are believed as a kind of low cost, nontoxic, and environment-friendly materials [14-19]. They can be applied in the removal of dyes, heavy metal ions and other hazardous substances contained in industrial sewage. However, the application of untreated plant wastes as adsorbents can also bring several problems such as lower adsorption capacity, higher chemical oxygen demand (COD)

and biological chemical demand (BOD) as well as total organic carbon (TOC) due to release of soluble organic compounds contained in the plant materials [20]. Therefore, plant wastes need to be modified or treated before being applied for the decontamination of heavy metals and dyes. Furthermore, modification of agricultural by-products can be carried out to achieve adequate structural durability, enhance their natural ion exchange capability and add value to the by-product [21,22].

Surfactants are chemicals that have an amphiphathic structure with a hydrophobic tail and a hydrophilic head. Cationic surfactant was selected to modify agricultural byproduct to remove anionic ions or oil pollutants [23-26]. But a few investigations have been reported using wheat straw modified by surfactants for removal of anionic dyes from solution [27].

To the best of our knowledge, the application of sodium dodecyl sulfate (SDS) modified wheat straw for methylene blue (MB) removal from aqueous environment has not been reported so far. The aim of this work is to present and investigate an efficient methodology for color treatment by using modified adsorbent based on wheat straw immobilized anionic surfactant, sodium dodecyl sulfate (SDS), for the adsorptive removal of methylene blue (MB) as an example of cationic dyes. Optimization of all experimental controlling factors and conditions such as reaction contact time, pH, adsorbent dosage, initial dye concentration as well as mechanism of adsorption were also explored and evaluated.

***Corresponding author:** Ebrahimian Pirbazari A, Faculty of Fouman, College of Engineering, University of Tehran, Fouman, Iran and Faculty of Caspian, College of Engineering, University of Tehran, Rezvanshahr, Iran Tel: 43516-66456; E-mail: aebrahimian@ut.ac.ir

Received June 04, 2015; **Accepted** June 15, 2015; **Published** June 27, 2015

Citation: Azadeh EP, Seyed FH, Ardovan Y (2015) Surfactant-Modified Wheat Straw: Preparation, Characterization and its Application for Methylene Blue Adsorption from Aqueous Solution. J Chem Eng Process Technol 6: 231. doi:10.4172/2157-7048.1000231

Copyright: © 2015 Azadeh EP, et al. This is an open-access article distributed under the terms of the Creative Commons Attribution License, which permits unrestricted use, distribution, and reproduction in any medium, provided the original author and source are credited.

Experimental

Materials

The wheat straw (WS) used in this study was obtained from a local wheat field of Ardabil in Iran. The collected materials were washed several times with boiled water and finally with distilled water to remove any adhering dirt. The washed materials were then dried in the oven at 60°C for 48 h. The dried WS was then ground and sieved into a size range of 100-500 µm. Finally, the resulting product was stored in air-tight container for further use. The methylene blue (MB) purchased from Merck (No.115943), was selected as representative reactive dye for this study. A stock solution of MB was prepared by dissolving 1.0 g of MB in 1 L of deionized water, and the concentrations of MB used (50-500 mg/L) were obtained by dilution of the stock solution. The pH of the solution was adjusted to the desired value by adding a small quantity of 0.01M HCl or 0.01M NaOH. Sodium dodecyl sulfate (SDS) solutions were prepared from commercially available product (Merck, 8.22050) dissolved in distilled water.

Modification of WS by SDS and characterization

The solution of SDS was prepared below its critical micellar concentration (CMC=0.0082M), as beyond CMC the surface modification was not effective. 100 mL of 2×10^{-3} M SDS solution was treated with 10.0 g of WS and shaken in a temperature controlled shaker at 180 rpm for 3 h at 303K. The SDS-modified wheat straw (SMWS) was then filtered and washed with deionized water till conductance of filtrate was less than 0.05 µS. The SMWS was then dried in hot air oven at 80°C for 24 h. This was then stored in air tight container for further use.

Fourier transform infrared (FTIR) analysis was applied to determine the surface functional groups, using FTIR spectroscope (FTIR-2000, Bruker), where the spectra were recorded from 4000 to 400 cm⁻¹. Surface morphology was studied using Scanning Electron Microscopy (Vegall-Tescan Company). Specific surface area based on nitrogen physisorption was measured by Sibata surface area apparatus 1100. The samples were degassed at 100°C for 2 h prior to the sorption measurement.

Adsorption procedure

Equilibrium isotherms were determined by shaking a fixed mass of SMWS (0.2 g) with 100 mL of MB solutions with different initial concentrations (50, 100, 200, 300, 400 and 500 mg/L) in 250 mL glass Erlenmeyer's flasks at a temperature of 20°C and pH=7. The procedure was repeated for temperatures 30 and 40°C. Initial pH adjustments were carried out by adding either a 0.01M hydrochloric acid or 0.01M sodium hydroxide solution. After shaking the flasks at 180 rpm for 2 h, the reaction mixtures were filtered through filter paper, and then the filtrates were analyzed for the remaining MB concentrations with spectrometry at the wavelength of maximum absorbance, 664 nm using a double beam UV-Vis spectrophotometer (Shimadzu, Model UV2100, Japan).

Kinetic studies

Adsorption kinetics experiments were performed by contacting 200 mL MB solution of different initial concentrations ranging from 50 to 200 mg/L with 0.4 g SMWS in a 500 mL stopper red conical flask at room temperature. At fixed time intervals, the samples were taken from the solution and were analyzed.

Isotherm modeling

The non-linear forms of the Langmuir and Freundlich, isotherm models were used to analyze the equilibrium isotherm data [28]. The fitness of these models was evaluated by the non-linear coefficients of determination (R²). The Matlab (version 7.3) software package was used for the computing. The Langmuir adsorption isotherm assumes that adsorption takes place at specific homogeneous sites within the adsorbent and has found successful application for many processes of monolayer adsorption. The Langmuir isotherm can be written in the form:

$$q_e = (Q_{max} K_L C_e) / (1 + K_L C_e) \quad (1)$$

Where q_e is the adsorbed amount of the dye, C_e is the equilibrium concentration of the dye in solution, Q_{max} is the monolayer adsorption capacity and K_L is Langmuir adsorption constant. The Freundlich isotherm is an empirical equation which assumes that the adsorption occurs on heterogeneous surfaces. The Freundlich equation can be expressed as:

$$q_e = K_F C_e^{1/n} \quad (2)$$

Where K_F and $1/n$ are fitting constants which can be regarded roughly, the capacity and strength of adsorption, respectively.

Kinetic models

The Lagergren rate equation [29] is one of the most widely used adsorption rate equations for the adsorption of solute from a liquid solution. The pseudo-first-order kinetic model of Lagergren may be represented by:

$$\frac{dq}{dt} - q = k_1 t \quad (3)$$

Integrating this equation for the boundary conditions $t=0$ to $t=t$ and $q=0$ to $q=q_t$, gives:

$$\ln(q_e - q_t) = \ln q_e - k_1 t \quad (4)$$

Where q_e and q_t are the amounts of adsorbate (mg/g) at equilibrium and at time t (min), respectively, and k_1 is the rate constant of pseudo-first-order adsorption (min⁻¹). The validity of the model can be checked by linearized plot of $\ln(q_e - q_t)$ versus t . Also, the rate constant of pseudo-first-order adsorption is determined from the slope of the plot.

The pseudo-second-order equation based on adsorption equilibrium capacity can be expressed as:

$$1 / (q_e - q_t) - 1 / q_e = k_2 t \quad (5)$$

Taking into account, the boundary conditions $t=0$ to $t=t$ and $q=0$ to $q=q_t$, the integrated linear form the above equation can be rearranged to follow equation:

$$1 / (q_e - q_t) - 1 / q_e = k_2 t \quad (6)$$

Rearranging the variables gives the following equation:

$$t / q_t = 1 / k_2 q_e^2 + t / q \quad (7)$$

Where the theoretical equilibrium adsorption capacity (q_e) and the second-order constants k_2 (g mg⁻¹ min⁻¹) can be determined experimentally from the slope and intercept of plot t/q_t versus t .

Statistical analysis

All experiments were performed in duplicate and the mean values were presented. The data were analyzed by one-way analysis of variance

(ANOVA) using SPSS 11.5 for Windows. The data was considered statistically different from control at $P < 0.05$.

Studies on point zero charge (pH_{pzc})

In pH_{pzc} determination, 0.01M NaCl was prepared and its pH was adjusted in the range of 2-11 by adding 0.01M NaOH or HCl. Then, 50 mL of 0.01M NaCl each was put in conical flask and then 0.1 g of the SMRS was added to these solutions. These flasks were kept for 72 h and final pH of the solution was measured by using pH meter. Graphs were then plotted for pH_{final} versus $\text{pH}_{\text{initial}}$.

Result and Discussion

FTIR analysis

The FTIR technique is an important tool to identify some characteristic functional groups, which are capable of adsorbing metal ions and dye ions. Figure 1 was shown the FTIR of WS and SMWS before and after MB adsorption.

As shown in Figure 1, the spectra displayed a number of absorption peaks, indicating the complex nature of the material. The broad absorption peaks around 3588 cm^{-1} (Figure 1a) were indicative of the existence of bonded hydroxyl groups on the surface of wheat straw. This band was due to vibration of the silanol group; hydroxyl group linked in cellulose and lignin, and adsorbed water on the straw surface. The peaks observed at 2926 and 1363 cm^{-1} were assigned to the stretch vibration and bending vibration of C-H bond in methyl group, respectively. The peaks located at 1741 and 1516 cm^{-1} were characteristics of carbonyl group stretching from aldehydes and ketones [30]. These groups can be conjugated or non-conjugated to aromatic rings (1516 and 1741 cm^{-1} , respectively). The peak near 1425 cm^{-1} was also attributed to stretch vibration of C-O from carboxyl group. The peaks associated with the stretch vibration in aromatic rings were verified at 1603 and 1511 cm^{-1} while deformations related to C-H and C-O bonds were observed from 1085 to 1015 cm^{-1} . The strong C-O band at 1015 cm^{-1} also confirms the lignin structure of the wheat straw. The peak at 1222 cm^{-1} may be from the stretch vibration of C-O in phenols.

FT-IR spectrum of the SMWS (Figure 1b) shows more intense vibrations compare to WS at 3599 and 2900 cm^{-1} assigned to the $-\text{CH}_2$ group from SDS and the peak observed at 1244 cm^{-1} could be assigned to $-\text{SO}_3$ stretching vibration [31], and these suggest that the SDS have been successfully modified the surface of WS. However, the FT-IR spectra of SMWS and SMWS after MB adsorption were found to exhibit similar functional groups due to the domination of the functional groups of WS in this sorbent as the major component in these materials.

SEM and nitrogen physisorption analysis

Scanning electron micrographs of WS, SMWS and SMWS after MB adsorption were shown in Figure 2. The morphology of this material can facilitate the adsorption of metals and dyes, due to the irregular surface of the straw, thus makes possible the adsorption of adsorbate in different parts of this material. It is evident from the obtained SEM images that surfactant modification is significantly responsible to alter the physico-chemical properties of the materials. Furthermore, the surface of SMWS is rougher than that of WS. So, based on the morphology, it can be concluded that this material presents an adequate morphological profile to retain metal and dye ions [30]. The surface of SMWS after MB adsorption (Figure 2c), however, shows that the surface of WS are covered with MB molecules. The specific surface area

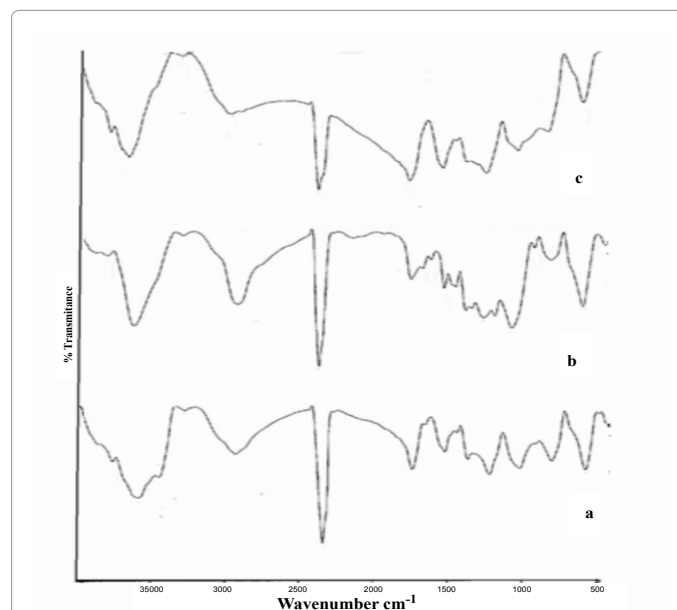


Figure 1: FTIR spectra of a) WS, b) SMWS and c) SMWS after MB adsorption.

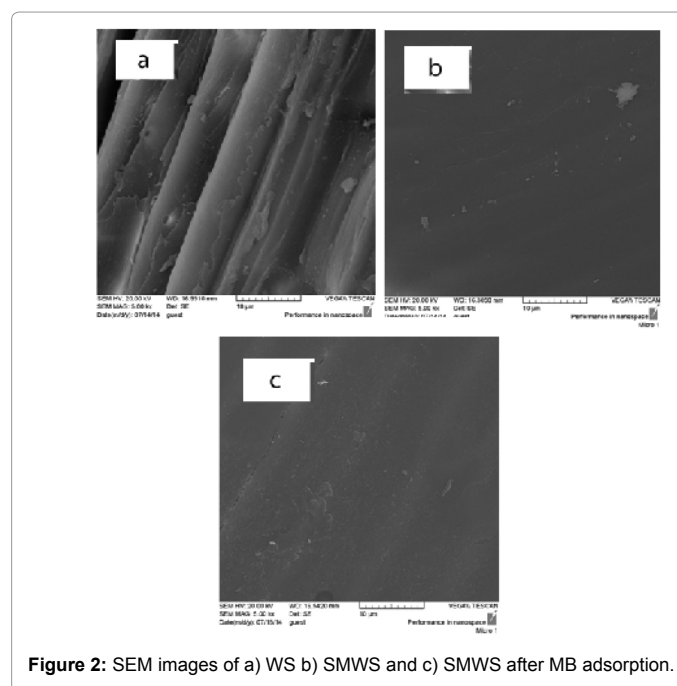


Figure 2: SEM images of a) WS b) SMWS and c) SMWS after MB adsorption.

of WS and SMWS based on nitrogen physisorption were determined by Brunauer-Emmett-Teller (BET) theory. It was found that the surface area of WS and SMWS were 45 and $130 \text{ m}^2 \text{ g}^{-1}$, respectively. As Nadeem and *et al.* reported [32], anionic (SDS) and cationic (CTAB) surfactant enhanced the characteristics of adsorbent better than the nonionic one (Triton X-100). The enhancement can be attributed to the typical properties of micelle formation, adsorption, wetting and solubilization. Being amphiphathic in nature, surfactant-modified surfaces can offer enhanced surface area and wetting (water or oil wet) according to the requirement because surfactant molecules are capable of organizing themselves accordingly. Moreover, the presence of electrostatic interactions facilitates the possibility for selective adsorption as well.

In mechanism section, we will give details about the role of surfactant in MB adsorption.

Effect of initial concentration and contact time on MB adsorption

Figure 3 shows the effect of the initial dye concentration (50-200 mg/L) on the adsorption of MB. It was observed that amount of MB adsorbed was rapid for the first 20 min and there after it proceeded at a slower rate (20-60 min) and finally reached saturation. The equilibrium adsorption increases from 8.90 to 28.86 mg/g, with increase in the initial MB concentration from 50 to 200 mg/L. The findings are because as the initial concentration increases, the mass transfer driving force becomes larger, hence resulting in higher MB adsorption [33]. It is also shown in Figure 3 that the contact time needed for MB solutions with initial concentrations of 50-200 mg/L to reach equilibrium was 60 min. The initial concentration provides an important driving force to overcome all mass transfer resistances of the MB between the aqueous and solid phase. However, the experimental data were measured at 120 min to be sure that full equilibrium was attained.

Point of zero charge (pH_{pzc}) studies and the effect of pH on MB adsorption

The point of zero charge (pH_{pzc}) is an important factor that determines the linear range of pH sensitivity and then indicates the type of surface active centers and the adsorption ability of the surface [34]. Many researchers studied the point of zero charge of adsorbents that prepared from agricultural solid wastes in order to better understand of adsorption mechanism. Cationic dye adsorption is favored at $pH > pH_{pzc}$, due to presence of functional groups such as OH, COO⁻ groups. Anionic dye adsorption is favored at $pH < pH_{pzc}$ where the surface becomes positively charged [35,36]. The graph of pH_{final} vs $pH_{initial}$ was plotted as shown in Figure 4. The intersections of the curves with the straight line are known as the end points of the pH_{pzc} , and this value is 8 for SMWS. Figure 5 shows the effect of pH on the adsorption of MB. The experiments were conducted at 50 mL of

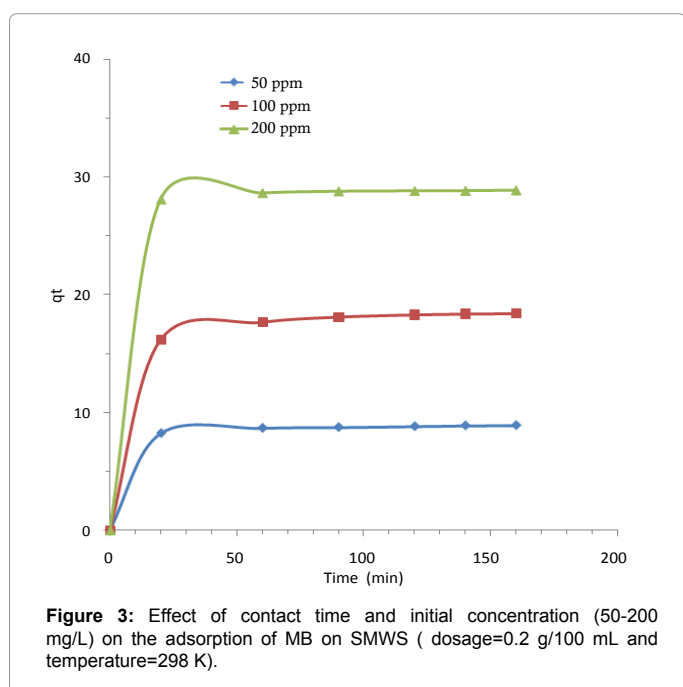


Figure 3: Effect of contact time and initial concentration (50-200 mg/L) on the adsorption of MB on SMWS (dosage=0.2 g/100 mL and temperature=298 K).

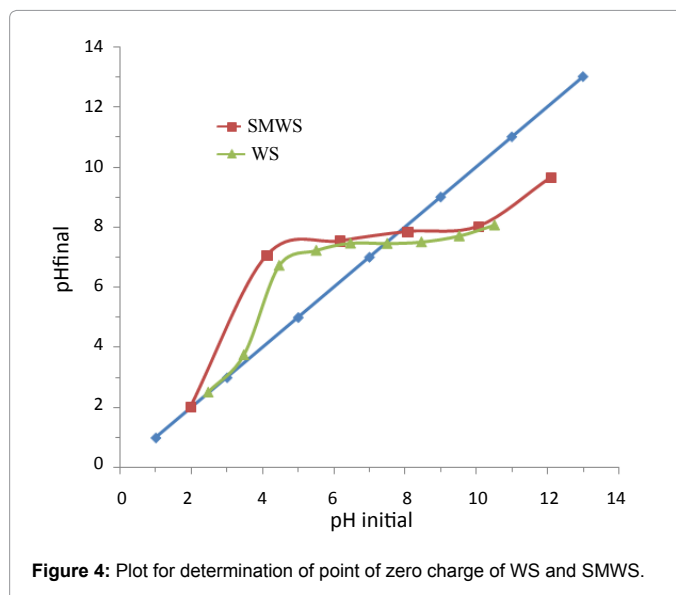


Figure 4: Plot for determination of point of zero charge of WS and SMWS.

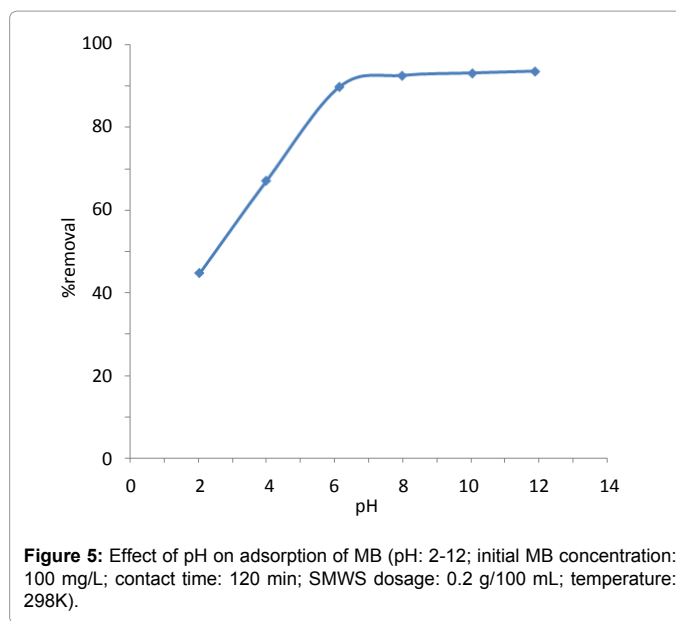


Figure 5: Effect of pH on adsorption of MB (pH: 2-12; initial MB concentration: 100 mg/L; contact time: 120 min; SMWS dosage: 0.2 g/100 mL; temperature: 298K).

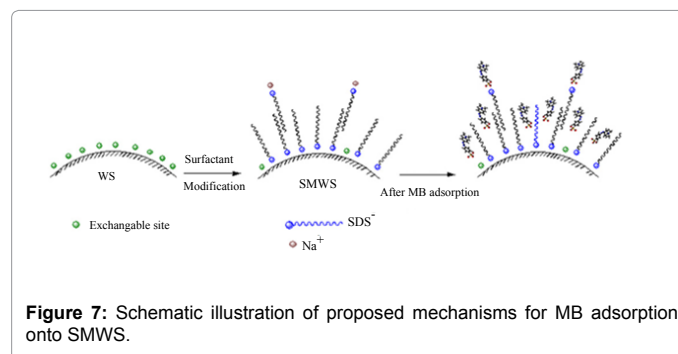
initial MB concentration, 0.10 g SMWS dose. It was observed that pH gives a significant influence to the adsorption process. MB is cationic dye, which exists in aqueous solution in the form of positively charged ions (MB⁺). As a charged species, the degree of its adsorption onto the adsorbent surface is primarily influenced by the surface charge on the adsorbent, which in turn is influenced by the solution pH. As shown in Figure 5, the removal percentage was minimum at pH 2 (44%), this increased up to 8 and remained nearly constant (92%) over the initial pH ranges of 8-12. This phenomenon occurred due to the presence of excess H⁺ ions in the adsorbate and the negatively charged surface adsorbent. Lower adsorption of MB at acidic pH ($pH < pH_{pzc}$) is due to the presence of excess H⁺ ions competing with the cation groups on the dye for adsorption sites. At higher solution pH ($pH > pH_{pzc}$), the SMWS possibly negatively charged and enhance the positively charged dye cations through electrostatic forces of attraction. We selected pH=8 for adsorption and kinetic experiments.

Effect of adsorbent dose

Adsorbent dose is an important parameter that strongly influences the adsorption process by affecting the adsorption capacity of the adsorbent [37]. Therefore, the influence of adsorbent dose on MB adsorption by SMWS was investigated in the range of 0.05-0.5 g/100 mL of MB solution (initial concentration: 100 mg/L, pH=8) (Figure 6). The adsorption efficiency increased from 85% to 96% as the adsorbent dose increased from 0.05 to 0.2 g. The increase in the percentage of dye removal with adsorbent dose could be attributed to an increase in the adsorbent surface area, augmenting the number of adsorption sites available for adsorption, as previously reported [38,39]. The decrease in sorption capacity with increasing dosage of adsorbent at constant dye concentration and volume may be attributed to saturation of adsorption sites due to particulate interaction such as aggregation [40]. Such aggregation would lead to a decrease in total surface area of the adsorbent and an increase in diffusional path length [41]. Therefore, in the following experiments, the adsorbent dose was fixed at 0.2 g/100 mL.

Mechanism of MB adsorption onto SMWS

The surface modification and proposed mechanism of MB adsorption onto SMWS is shown schematically in Figure 7. In oxides, generally, a monolayer of surfactant molecules (which is called hemimicelles) is formed with the surfactant head group facing toward the oxide surface and its hydrocarbon tail groups into solution. In the event that higher concentrations of the surfactant molecules are presented in the solution, new hydrophobic interactions between hydrocarbons tail-groups will be occurred which results in the formation of discrete surface aggregates termed admicelles. Both of these hemimicelle or admicelle regions formed on the surface of oxides are potential adsorbing locations [38]. Another possible mechanism is the hydrocarbons tail group of surfactant may interact with solid surface through hydrophobic-bonding and the head group directed toward the bulk of the solution, so the surface is potential negative or positive. The mechanism was due to adsorption of SDS onto WS surface (Figure 7). The non-polar portion (alkyl) of SDS may interact with WS surface through hydrophobic-bonding and the polar (negative



charged) head group directed toward the bulk of the solution, so the surface is potential negative. So there is negative charge onto surface of SMWS and the mechanism of adsorption about MB onto SMWS may include electrostatic interaction or ion-exchange. Also, some of the MB molecules adsorbed onto the SMWS surface through hydrophobic interaction between MB and hydrocarbon tail of surfactant (Figure 7).

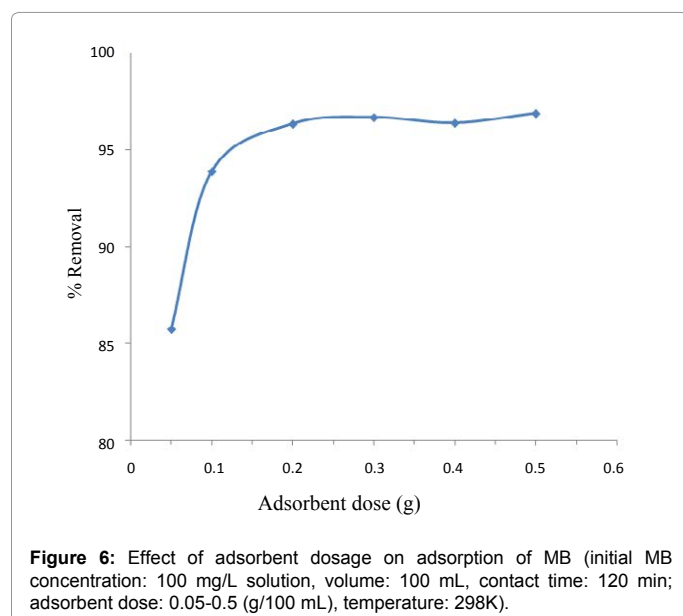
Isotherm modeling

Figure 8 and Table 1 show the fitting parameters for the measured isotherm data for MB adsorption onto SMWS in the nonlinear forms of the Langmuir and Freundlich models. By comparing the correlation coefficients R^2 , it can be deduced that the experimental equilibrium adsorption data are well described by the Langmuir equation compared with Freundlich model. This suggests the monolayer coverage of the surface of SMWS by MB molecules. The high adsorption capacity in SMWS could be due to the large amount of surfactant on the surface of WS particles, which could result in increasing amounts of negatively charged sites on the surface of WS and finally facilitates the attraction towards the positively dye molecules. Moreover, the Q_{max} decreases with an increase in temperature (from 303K to 323K), which specifies an exothermic nature of the existing process.

The Freundlich equation is suitable for homogeneous and heterogeneous surfaces, indicating a multilayer adsorption [39]. The magnitude of the Freundlich constant n gives a measure of favorability of adsorption. Values of $n > 1$ represent a favorable adsorption process [37]. For the present study, the value of n also presents the same trend at all the temperatures indicating the favorable nature of adsorption of MB by SMWS.

Adsorption kinetics studies

The dynamics of the adsorption can be studied by the kinetics of adsorption in terms of the order of the rate constant [40]. The adsorption rate is an important factor for a better choice of material to be used as an adsorbent; where the adsorbent should have a large adsorption capacity and a fast adsorption rate. Most of adsorption studies used pseudo-first-order and pseudo-second-order models to study the adsorption kinetics. For the pseudo-first-order model, the adsorption rate was expected to be proportional to the first power of concentration, where the adsorption was characterized by diffusion through a boundary. The pseudo-first-order model sometimes does not fit well for the whole range of contact time when it failed theoretically to predict the amount of dye adsorbed and thus deviated from the theory. In that case, the pseudo-second-order equation used was based on the sorption capacity of the solid phase, where the pseudo-second-order model assumes that chemisorptions may be the rate-controlling step in the adsorption processes [41]. The transient behavior of the



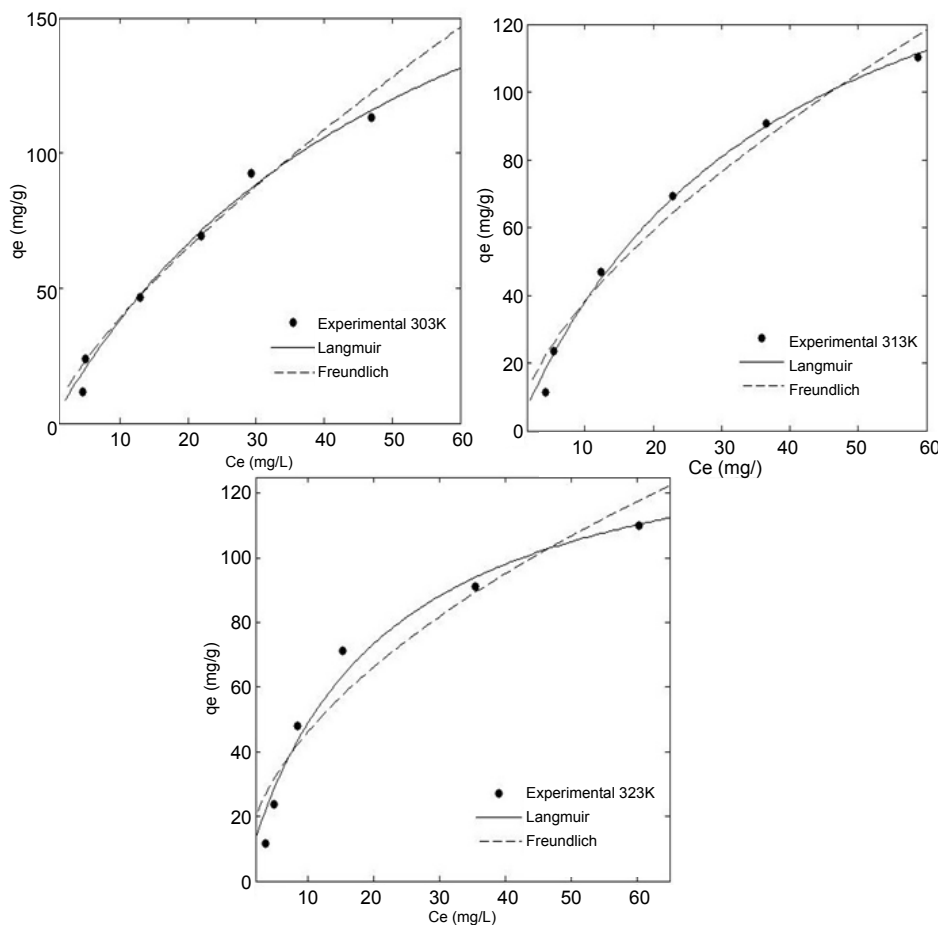


Figure 8: Isotherm plots for MB (initial concentration=50-500 mg/L, SMWS dosage=0.2 g/100 mL, contact time= 120 min) adsorption onto SMWS at different temperatures.

MB adsorption process was analyzed by using the pseudo-first and pseudo-second-order kinetic models. Plotting $\ln(q_e - q_t)$ against t permits calculation of k_1 (Figure 9a). The rate constants, k_1 , evaluated from these plots with the correlation coefficients obtained are listed in Table 2. Plotting t/q against t (Figure 9b), gives a straight line where k_2 can be calculated. Usually the best-fit model can be selected based on the linear regression correlation coefficient R^2 values. Generally the kinetic adsorption is better represented by pseudo-second-order model for anionic and cationic dye adsorption. The R^2 listed (Table 2) for the pseudo-first-order kinetic model was between 0.9376 and 0.9852. The R^2 values for pseudo-second-order model were close to 1, which is higher than the R^2 values obtained for the pseudo-first-order model. Therefore, the adsorption kinetics could well be satisfactorily more favorably described by pseudo-second-order kinetic model for MB adsorption onto SMWS.

In adsorption process of dye ion on the solid surface, the dye species migrate towards the surface of the adsorbent. This type of migration proceeds till the concentration of the adsorbate species, adsorbed, on to the surface of the adsorbent. Once equilibrium is attained, the migration of the solute species from the solutions tops. Under this situation, it is possible to measure the magnitude of the distribution of the solute species between the liquid and solid phases. The magnitude of this kind of distribution is a measure of the efficiency of the chosen adsorbent in the adsorbate species. When a powdered

solid adsorbent material is made in contact with a solution containing dyes, the dyes first migrate from the bulk solution to the surface of the liquid film. This surface exerts a diffusion barrier. This barrier may be very significant or less significant [42]. The involvement of a significant quantum of diffusion barrier indicates the dominant role taken up by the film diffusion in the adsorption process. Furthermore, the rate of an adsorption process is controlled either by external diffusion, internal diffusion or by both types of diffusions. The external diffusion controls the migration of the solute species from the solution to the boundary layer of the liquid phase. However, the internal diffusion controls the transfer of the solute species from the external surface of the adsorbent to the internal surface of the pores of the adsorbent material [43]. It is now well established, that during the adsorption of dye over a porous adsorbent, the following three consecutive steps were taken place [44,45]:

- (i) Transport of the ingoing adsorbate ions to external surface of the adsorbent (film diffusion).
- (ii) Transport of the adsorbate ions within the pores of the adsorbent except for a small amount of adsorption, which occurs on the external surface (particle diffusion).
- (iii) Adsorption of the ingoing adsorbate ions on the interior surface of the adsorbent.

Langmuir			
Temperature (K)	303	313	323
Q_{max} (mg/g)	126.60	120.48	119.05
K_L (L/mg)	0.0114	0.0126	0.0133
R^2	0.9919	0.9902	0.9905
Freundlich			
Temperature (K)	303	313	323
n	1.209	1.207	1.234
k_F (mg/g) (dm ³ /mg) ^{1/n}	1.842	1.882	2.042
R^2	0.9662	0.9732	0.9719

Table 1: Isotherm parameters for MB adsorption (initial concentration=50-500 mg/L, SMWS dosage=0.2 g/100 mL, contact time=120 min) onto SMWS.

C_0 (mg/L)	Pseudo-first order			Pseudo-second order		
	q_e (mg/g)	k_1 (1/min)	R^2	q_e (mg/g)	k_2 (g/mg.min)	R^2
50	1.158	0.0242	0.9376	9.033	0.0485	0.9999
100	5.040	0.0334	0.9848	18.832	0.0153	1.000
200	1.137	0.0256	0.9852	68.985	0.0522	1.000

Table 2: Kinetic parameters for the adsorption of MB (initial concentration=50-200 mg/L, SMWS dosage=0.2 g/100 mL and temperature=298K) onto SMWS based on Lagergren rate equation.

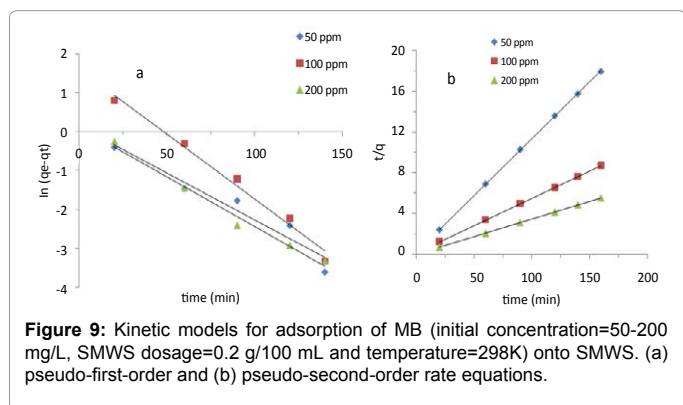


Figure 9: Kinetic models for adsorption of MB (initial concentration=50-200 mg/L, SMWS dosage=0.2 g/100 mL and temperature=298K) onto SMWS. (a) pseudo-first-order and (b) pseudo-second-order rate equations.

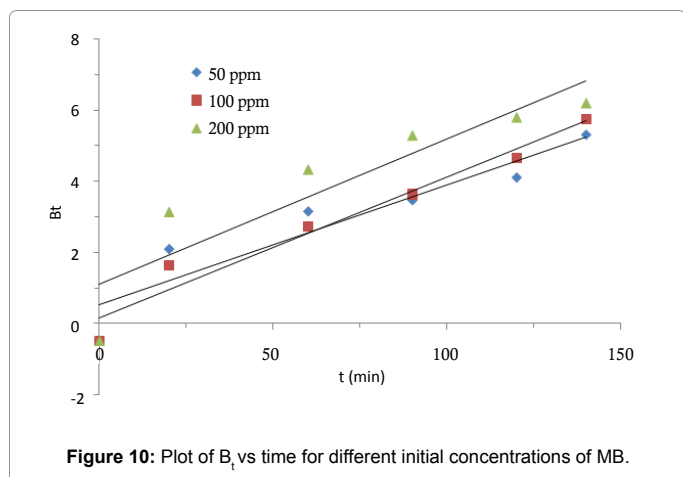


Figure 10: Plot of B_t vs time for different initial concentrations of MB.

Out of these three processes, the third process is considered to be very fast and is not the rate limiting step in the uptake of organic compounds. The remaining two steps impart the following three possibilities:

Case 1: External transport > internal transport, where rate is governed by particle diffusion.

Case 2: External transport < internal transport, where the rate is governed by film diffusion.

Case 3: External transport \approx internal transport, which accounts for the transport of the adsorbate ions to the boundary and may not be possible with in a significant rate, which later on gives rise to the formation of a liquid film surrounded by the adsorbent particles with a proper concentration gradient. In order to predict the actual slow step involved in the adsorption process, the kinetic data were further analyzed using the Boyd model given by Eq. (7) [46].

$$B_t = -0.4977 - \ln(1 - F) \quad (7)$$

F represents the fraction of solute adsorbed at anytime, t (h), as calculated using Eq. (8)

$$F = q_t / q_e \quad (8)$$

Where q_t and q_e are amounts adsorbed after time t and after infinite time (150 min), respectively. The calculated B_t values were plotted against time t (min), as shown in Figure 10. The plot of B_t vs time distinguishes between the film-diffusion and particle-diffusion-controlled rates of adsorption. The linear lines for all MB initial concentrations did not pass through the origin and the points were scattered. This indicated that the adsorption of MB on the SMWS was mainly governed by external mass transport where particle diffusion was the rate limiting step [46].

Desorption studies of MB

Desorption studies can help enlightening the mechanism of an adsorption process. If the dye adsorbed onto the adsorbent can be desorbed by water, it can be said that the attachment of the dye onto the adsorbent is by weak bonds. If the strong bases, such as NaOH can desorb the dye, it can be said that the attachment of the dye onto the adsorbent is by ion exchange [47,48]. Hence, neutral distilled water was used in the elution of MB molecules from the SMWS followed by NaOH solution. The percentage of desorption obtained were 15% and 20% for using neutral distilled water and 0.1M NaOH solution, respectively. The fact that the low desorption occurred with distilled water and NaOH solution suggests that adsorption of MB onto SMWS carries out significantly by another mechanism. The mode of existence of surfactant molecules on solid surface has been investigated widely [38]. As we mentioned above, a possible mechanism is the hydrocarbons tail group of surfactant may interact with solid surface through hydrophobic-bonding and the head group directed toward the bulk of the solution, so the surface is potential negative or positive. Consequently, it can be conceived from the result of desorption by NaOH that some surfactant molecular arrange in this manner in the research. Here, the above conclusion related to ion-exchange mechanism is clearly confirms. Taking all the results that have been discussed above into account, it is proposed that enhanced hydrophobic interaction is the predominant mechanism contributing to the increased MB adsorption on the SMWS, followed by a certain amount of the cationic exchange. For better illustration of the process of adsorption, a suggested adsorption structure was shown in Figure 7.

Conclusion

The results of this investigation show that sodium dodecyl sulfate modified wheat straw (SMWS) has excellent adsorption capacity for the removal of methylene blue from aqueous solutions. SEM shows that morphological feature of WS changed after modification. FTIR and SEM results suggest that the SDS have been successfully coated the surface of WS. The adsorption isotherm experiment was conducted

at different temperatures (303, 313 and 323K), and it was found that the uptake of MB decreased with increasing temperature and hence adsorption process is exothermic in nature. The equilibrium data were analyzed by the Langmuir and Freundlich models and the Langmuir model was found to fit the equilibrium data better. The pseudo-second order kinetic model agrees very well with the dynamic behavior for the adsorption of MB onto surfactant modified wheat straw. The desorption studies implied that the hydrophobic interaction and cationic exchange models controlled simultaneously during the adsorption process, but the former is a dominant mechanism. The developed SMWS not only has demonstrated higher adsorption efficiency and fast kinetics but also have shown additional benefits like cost-effectiveness and environmental-friendliness. It can be concluded to be a promising advanced adsorbent in environmental pollution cleanup.

Acknowledgment

The authors wish to acknowledge the financial support of the University of Tehran.

References

1. Doney SC (2010) The growing human footprint on coastal and open-ocean biogeochemistry. *Science* 328: 1512-1516.
2. Neill CO, Hawkes FR, Hawkes DL, Lourenco ND, Pinheiro HM, et al. (1999) Colour in textile effluents – sources, measurement, discharge consents and simulation: a review. *J Chem Technol Biotechnol* 74: 1009-1018.
3. Crini G (2006) Non-conventional low-cost adsorbents for dye removal: a review. *Bioresour Technol* 97: 1061-1085.
4. Tan IA, Ahmad AL, Hameed BH (2008) Adsorption of basic dye on high-surface-area activated carbon prepared from coconut husk: equilibrium, kinetic and thermodynamic studies. *J Hazard Mater* 154: 337-346.
5. Vadivelan V, Kumar KV (2005) Equilibrium, kinetics, mechanism, and process design for the sorption of methylene blue onto rice husk. *J Colloid Interface Sci* 286: 90-100.
6. Seshadri S, Bishop PL, Agha AM (1994) Anaerobic/aerobic treatment of selected azo dyes in wastewater. *Waste Manag* 14: 127-137.
7. Guibal E, Roussy J (2007) Coagulation and flocculation of dye-containing solutions using a biopolymer (Chitosan). *React Funct Polym* 67: 33-42.
8. Malik PK, Saha SK (2003) Oxidation of direct dyes with hydrogen peroxide using ferrous ion as catalyst. *Sep Purif Technol* 31: 241-250.
9. Koch M, Yediler A, Lienert D, Insel G, Ketrup A (2002) Ozonation of hydrolyzed azo dye reactive yellow 84 (CI). *Chemosphere* 46: 109-113.
10. Rizzo L, Koch J, Belgiorio V, Anderson MA (2007) Removal of methylene blue in a photocatalytic reactor using polymethylmethacrylate supported TiO₂ nanofilm. *Desalination* 211: 1-9.
11. Arslan I, Balciolu IA (1999) Degradation of commercial reactive dyestuffs by heterogeneous and homogenous advanced oxidation processes: a comparative study. *Dyes and Pigments* 43: 95-108.
12. Ciardelli G, Corsi L, Marucci M (2000) Membrane separation for wastewater reuse in the textile industry. *Resour Conserv Recycl* 31: 189-197.
13. Venkata RB, Sastry CA (1987) Removal of dyes from water and wastewater by adsorption. *Ind J Environ Prot* 7: 363-376.
14. Farooq U, Kozinski JA, Khan MA, Athar M (2010) Biosorption of heavy metal ions using wheat based biosorbents—a review of the recent literature. *Bioresour Technol* 101: 5043-5053.
15. Oei BC, Ibrahim S, Wang S, Ang HM (2009) Surfactant modified barley straw for removal of acid and reactive dyes from aqueous solution. *Bioresour Technol* 100: 4292-4295.
16. Ibrahim S, Fatimah I, Ang HM, Wang S (2010) Adsorption of anionic dyes in aqueous solution using chemically modified barley straw. *Water Sci Technol* 62: 1177-1182.
17. Ibrahim S, Shuy WZ, Ang HM, Wang SB (2010) Preparation of bioadsorbents for effective adsorption of a reactive dye in aqueous solution. *Asia-Pac J Chem Eng* 5: 563-569.
18. Han FM, Peng ZH, Song W, Zhang HM, Zhu MM, et al. (2007) Identification of dauricine and its metabolites in rat urine by liquid chromatography-tandem mass spectrometry. *J Chromatogr B Analyt Technol Biomed Life Sci* 854: 1-7.
19. Yan H, Zhang WX, Kan XW, Dong L, Jiang ZW, et al. (2011) Sorption of methylene blue by carboxymethyl cellulose and reuse process in a next procedure. *Colloids Surf A* 380: 143-151.
20. Wan Ngah WS, Hanafiah MA (2008) Removal of heavy metal ions from wastewater by chemically modified plant wastes as adsorbents: a review. *Bioresour Technol* 99: 3935-3948.
21. O'Connell DW, Birkinshaw C, O'Dwyer TF (2008) Heavy metal adsorbents prepared from the modification of cellulose: a review. *Bioresour Technol* 99: 6709-6724.
22. Vaughan T, Seo CW, Marshall WE (2001) Removal of selected metal ions from aqueous solution using modified corn cobs. *Bioresour Technol* 78: 133-139.
23. Zhao BL, Xiao W, Shang Y, Zhu HM, Han RP (2014) Adsorption of light green anionic dye using cationic surfactant-modified peanut husk in batch mode. *Arab J Chem* (in press).
24. Su Y, Zhao B, Xiao W, Han R (2013) Adsorption behavior of light green anionic dye using cationic surfactant-modified wheat straw in batch and column mode. *Environ Sci Pollut Res Int* 20: 5558-5568.
25. Oei BC, Ibrahim S, Wang S, Ang HM (2009) Surfactant modified barley straw for removal of acid and reactive dyes from aqueous solution. *Bioresour Technol* 100: 4292-4295.
26. Zhang S, Zhang R, Xiao W, Han R (2013) Adsorption of chloro-anilines from solution by modified peanut husk in fixed-bed column. *Water Sci Technol* 68: 2158-2163.
27. Su YY, Jiao YB, Dou CC, Han RP (2013) Biosorption of methyl orange from aqueous solutions using cationic surfactant-modified wheat straw in batch mode. *Desalin Water Treat* 52: 6145-6155.
28. Liu Y, Liu YJ (2008) Biosorption isotherms, kinetics and thermodynamics. *Sep Purif Technol* 61: 229-242.
29. Lagergren S (1898) About the theory of so-called adsorption of soluble substances. *K Sven Vetenskapskad Handl* 24: 1-39.
30. Tarley CR, Arruda MA (2004) Biosorption of heavy metals using rice milling by-products. Characterisation and application for removal of metals from aqueous effluents. *Chemosphere* 54: 987-995.
31. Chen H, Zhao J, Wu J, Dai G (2011) Isotherm, thermodynamic, kinetics and adsorption mechanism studies of methyl orange by surfactant modified silkworm exuviae. *J Hazard Mater* 192: 246-254.
32. Nadeema M, Shabbir M, Abdullah MA, Shah SS, McKay G (2009) Sorption of cadmium from aqueous solution by surfactant-modified carbon adsorbents. *Chem Eng J* 148: 365-370.
33. Nasuha N, Hameed BH, Din AT (2010) Rejected tea as a potential low-cost adsorbent for the removal of methylene blue. *J Hazard Mater* 175: 126-132.
34. Poghossian AA (1997) Determination of the pH_{pzc} of insulators surface from capacitance-voltage characteristics of MIS and EIS structures. *Sens Actuator B: Chem* 44: 551-553.
35. Radovic LR, Silva IF, Ume JI, Menendez JA, Leon CA, et al. (1997) An experimental and theoretical study of the adsorption of aromatics possessing electron-withdrawing and electron-donating functional groups by chemically modified activated carbons. *Carbon* 35: 13390-1348.
36. Savova D, Petrov N, Yardim MF, Ekinci E, Budinova T, et al. (2003) The influence of the texture and surface properties of carbon adsorbents obtained from biomass products on the adsorption of manganese ions from aqueous solution. *Carbon* 41: 1897-1903.
37. Aksakal O, Uzun H (2010) Equilibrium, kinetic and thermodynamic studies of the biosorption of textile dye (Reactive Red 195) onto *Pinus sylvestris* L. *J Hazard Mater* 181: 666-672.
38. Crini G, Peindy HN, Gimbert F, Robert C (2007) Removal of C.I. Basic Green 4 (Malachite Green) from aqueous solutions by adsorption using cyclodextrin-based adsorbent: kinetic and equilibrium studies. *Sep Purif Technol* 53: 97-110.
39. Ariapad A, Zanjanchi MA, Arvand M (2012) Efficient removal of anionic surfactant using partial template-containing MCM-41. *Desalination* 284: 142-149.

40. Igwe JC, Abia AA (2010) Maize cob and husk as adsorbent for removal Cd, Pb and Zn ions from wastewater. *Phys Sci* 2: 83-94.
41. Gómez V, Larrechi MS, Callao MP (2007) Kinetic and adsorption study of acid dye removal using activated carbon. *Chemosphere* 69: 1151-1158.
42. Aksu Z (2005) Application of biosorption for the removal of organic pollutants: a review. *Process Biochem* 40: 997-1026.
43. Gupta VK, Mittal A, Gajbe V (2005) Adsorption and desorption studies of a water soluble dye, Quinoline Yellow, using waste materials. *J Colloid Interface Sci* 284: 89-98.
44. Gupta VK, Ali I, Suhas, Mohan D (2003) Equilibrium uptake and sorption dynamics for the removal of a basic dye (basic red) using low-cost adsorbents. *J Colloid Interface Sci* 265: 257-264.
45. Missel PJ (2000) Finite element modeling of diffusion and partitioning in biological systems: the infinite composite medium problem. *Ann Biomed Eng* 28: 1307-1317.
46. Weber WJ, Morris JC (1963) Kinetics of adsorption on carbon from solution. *J Sanit Eng Div* 89: 31-60.
47. Tan IAW, Hameed BH (2010) Adsorption isotherms, thermodynamics and desorption studies of basic dye on activated carbon derived from oil palm empty fruit bunch. *J Appl Sci* 10: 2565-2571.
48. Mall ID, Srivastava VC, Kumar GVA, Mishra IM (2006) Characterization and utilization of mesoporous fertilizer plant waste carbon for adsorptive removal of dyes from aqueous solution. *Colloids Surf A: Physicochem Eng Aspects* 278: 175-187.